# The F.E.M. study concerning the influence of air humidity about the dynamical flow around the spatial petroleum coke plant

Mihai D.L. Țălu, Ștefan D.L. Țălu and Marin Bică

*Abstract*— The goal of this study was to investigate the influence of air humidity variation concerning the dynamical flow around of a petroleum coke plant. A finite element program was used for numerical analysis and partial results was exposed and compared with the experimental measurements. The 3D model of plant can be adapted for appropriate CAD applications.

*Keywords -* Dynamical air flow, Finite element method (F.E.M.), humidity, petrochemistry petroleum coke plant.

## I.  INTRODUCTION

ON the Romanian petrochemistry industry the production of the petroleum coke plant through the tardy method is usually metting. In this sense as example is given the installation built on the petrochemistry industrial platforms of Onesti.

This plant works from 1996 in continuous regime, in cycles by forty-eight hours, with three hundred eighty-five tones production on cycle, [12].

A direction from the design activity takes into consideration the influence of the aerodynamically flow around the spatial body of plant which engendering the stress and deformation of structure beside the other important loadings.

In present paper the influence of air humidity variation concerning the dynamical flow is scrupulously theoretical investigated and partial results was exposed comparative with the experimental measurements.

Mihai D.L. Țălu is with the University of Craiova, Romania. He is now with the Department of Applied Mechanics, Faculty of Mechanics, 165 Calea Bucuresti Street, Craiova, 200585 Romania (phone: +40-251-418-803; fax: +40-251-418-803; e-mail: mihai_talu@yahoo.com).

Ștefan D.L. Țălu is with the Technical University of Cluj-Napoca, Romania. He is now with the Department of Descriptive Geometry and Engineering Graphics, Faculty of Mechanics, 103-105 B-dul Muncii Street, Cluj-Napoca, 400641 Romania (e-mail: stefan_ta@yahoo.com).

Marin Bică is with the University of Craiova, Romania. He is now with the Department of Road Vehicles, Faculty of Mechanics, 165 Calea Bucuresti Street, Craiova, 200585 Romania (phone: +40-251-418-803; fax: +40-251-418-803; e-mail: mbica@mecanica.ucv.ro).

The theoretical method to study this problem is the Finite Element Method.

## II.  THE SPATIAL MODEL OF PLANT

The 3D model of plant is in detail presented in paper [15] and this is made with aid of Solid Works 2007 software [18].

The real dimensional sizes of plant are big 28 x 6 x 6 $m^3$ and the structure is also complex. In Fig. 1 is given the isometric view of the installation on is marked the important elements of installation.
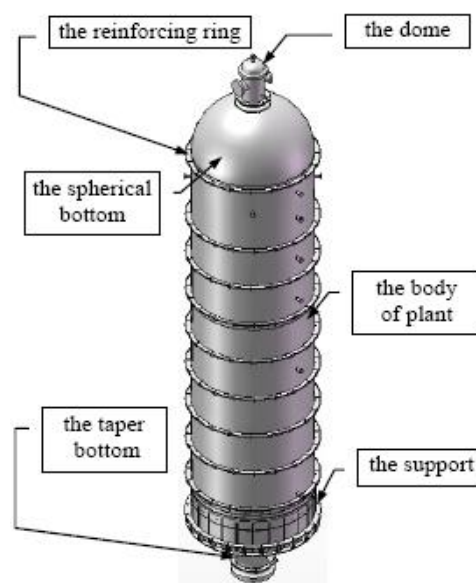


Fig. 1. The isometric view of the petroleum coke plant

## III.  THE EXPERIMENTAL MEASUREMENTS

To investigate the fields of physical properties of air in the dynamical flow was placed in the adjacent surface of plant a numbers of twenty-three sensors connected to a Multilyzer analyzer.

These sensors are mounted in two planes at levels of the reinforcing rings in concordance with Fig. 2:
- on points $P_{19}$, .., $P_{23}$, in Plane 1 placed in front of plant;
- on points $P_{19}$, .., $P_{23}$, in Plane 1 placed behind of plant;

- on points $P_{10}$, .., $P_{18}$, in Plane 2 placed on lateral of plant;

– the deviation of temperature in plots from Fig. 9 to Fig. 11;
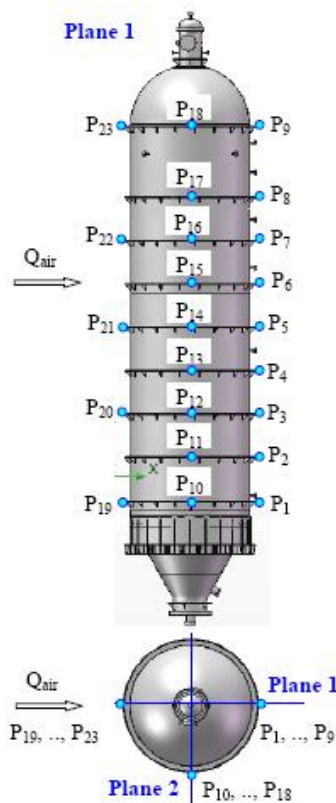– the deviation of density in plots from Fig. 12 to Fig. 14.



Fig. 2. The position of the Multilyzer's sensors on the plant

## IV. THE THEORETICAL ANALYSIS WITH THE F.E.M. OF THE AERODYNAMICAL FLOW

### 4.1 The initial data for numerical simulation

The study of the dynamical flow as consequence of humidity variation is made with aid of Cosmos Flow 2007 software, [19].
The initial data of external flow used in simulation are:
– the incident angle of the air with structure, $\alpha = 90°$;
– the physical parameters which characterize the initial front of air: p = 90330 [Pa], T = 16 [°C], v = 34,5 [m/s], $\varphi = 0 \div 100$ [%].

### 4.2. The results of simulation

### 4.2.1. The graphical results obtained with the F.E.M.

To compact the numerical results of study at levels of points $P_1$ to $P_{23}$ is determined the value of deviation for physical parameters with humidity variation comparative with the case of no humidity. Each label attached of plots gives the detailed specifications concerning the results presented, thus:
– the deviation of velocity in plots from Fig. 3 to Fig. 5;
– the deviation of pressure in plots from Fig. 6 to Fig. 8;
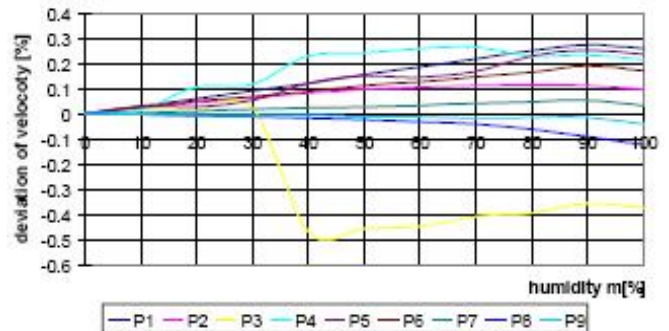


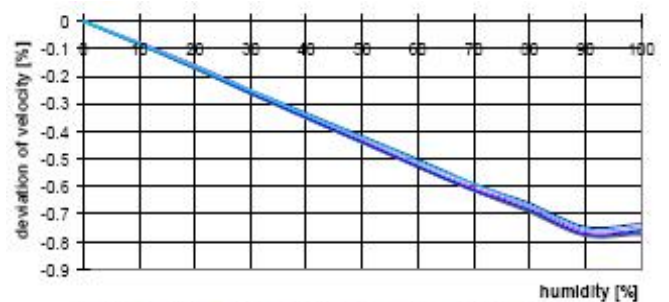Fig. 3. The deviation of velocity calculated in points $P_1$ to $P_9$



Fig. 4. The deviation of velocity calculated in points $P_{10}$ to $P_{18}$
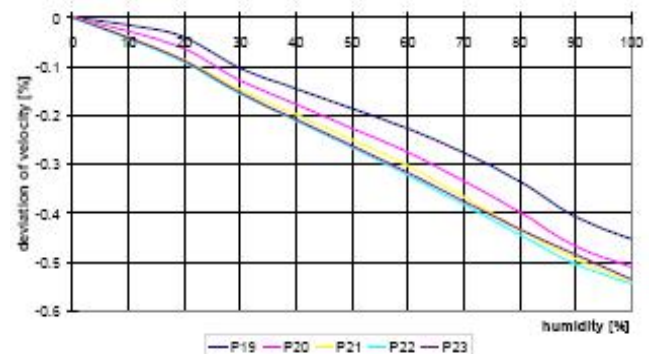


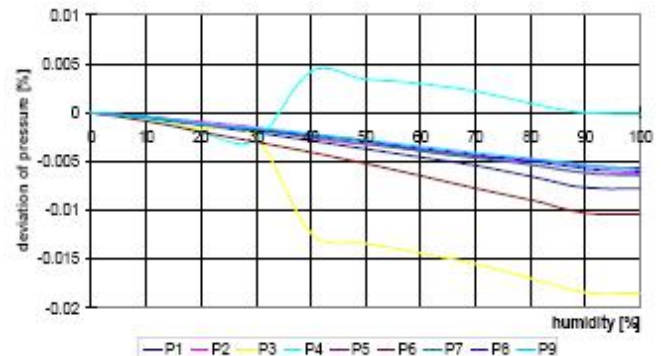Fig. 5. The deviation of velocity calculated in points $P_{19}$ to $P_{23}$



Fig. 6. The deviation of pressure calculated in points $P_1$ to $P_9$
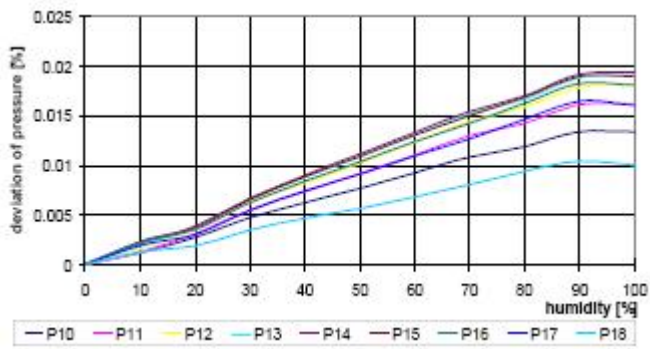
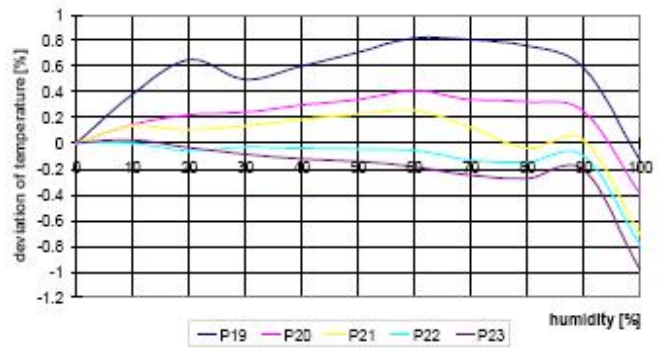Fig. 7. The deviation of pressure calculated in points $P_{10}$ to $P_{18}$



Fig. 11. The deviation of temperature calculated in points $P_{19}$ to $P_{23}$
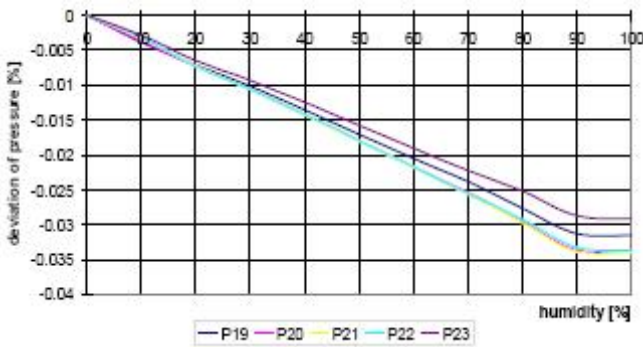


Fig. 8. The deviation of pressure calculated in points $P_{19}$ to $P_{23}$
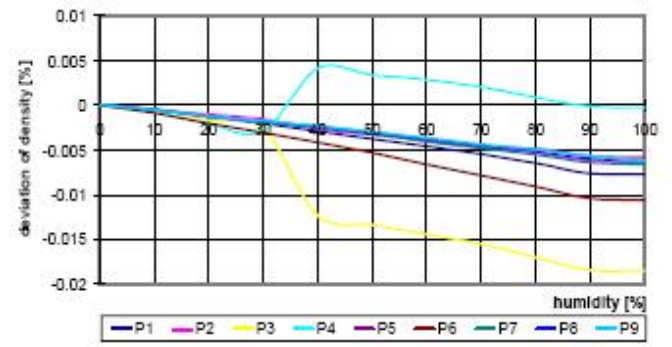


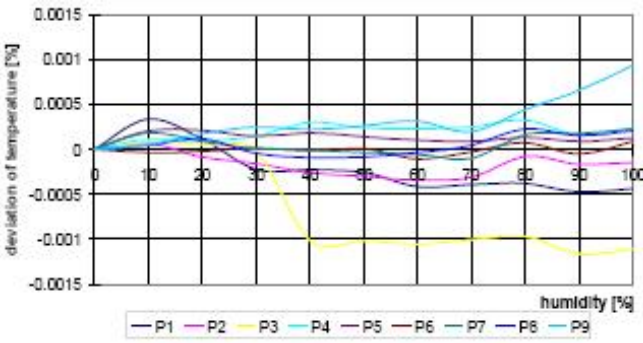Fig. 12. The deviation of density calculated in points $P_1$ to $P_9$



Fig. 9. The deviation of temperature calculated in points $P_1$ to $P_9$
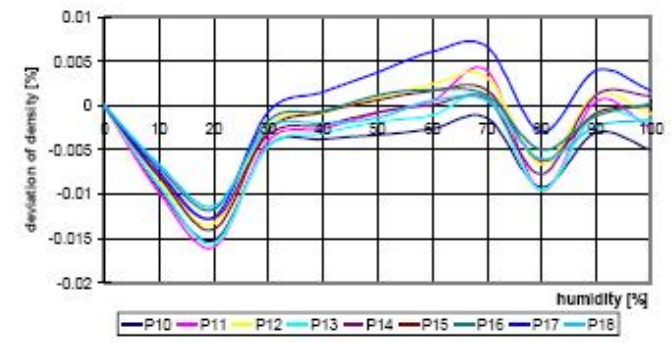


Fig. 13. The deviation of density calculated in points $P_{10}$ to $P_{18}$
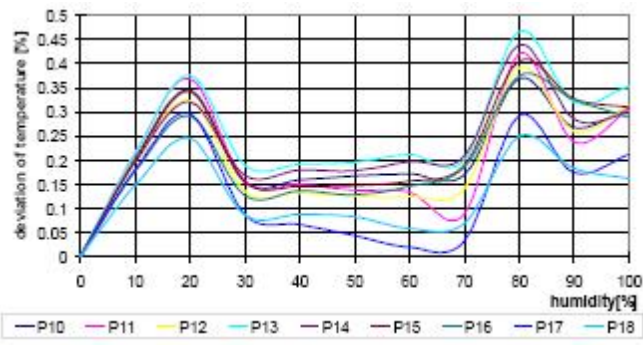


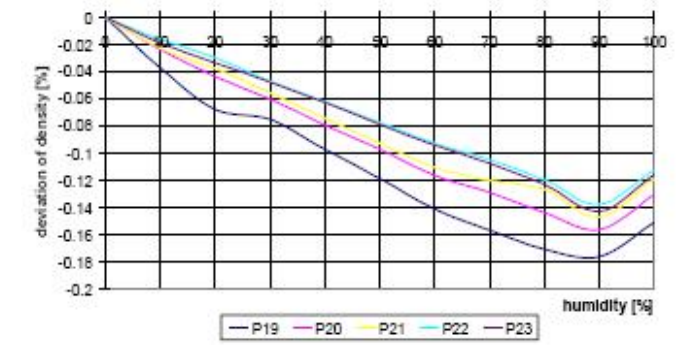Fig. 10. The deviation of temperature calculated in points $P_{10}$ to $P_{18}$



Fig. 14. The deviation of density calculated in points $P_{19}$ to $P_{23}$

The 3D fields of physical sizes calculated through numerical simulation at $\varphi = 40$ [%], (which can be comparated with the experimental measurements presented in this paper), on surfaces of plant are given in Fig.15 to Fig.18.
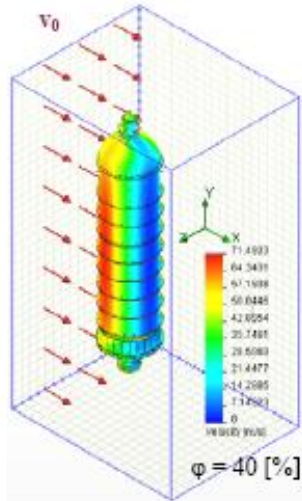


Fig. 15. The 3D field of velocity on surfaces of plant



Fig. 16. The 3D field of pressure on surfaces of plant
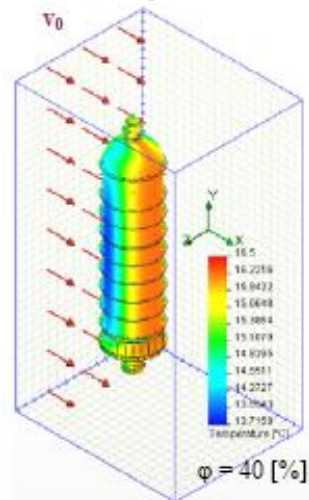


Fig. 17. The 3D field of temperature on surfaces of plant



Fig. 18. The 3D field of density on surfaces of plant

In Fig. 19 to Fig. 26 are given the fields contours and isolines of distributions for velocity, pressure, temperature and density on plane $P_1$ and $P_2$.
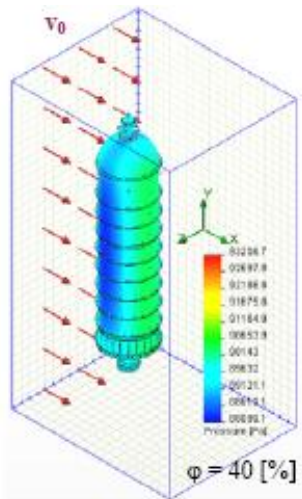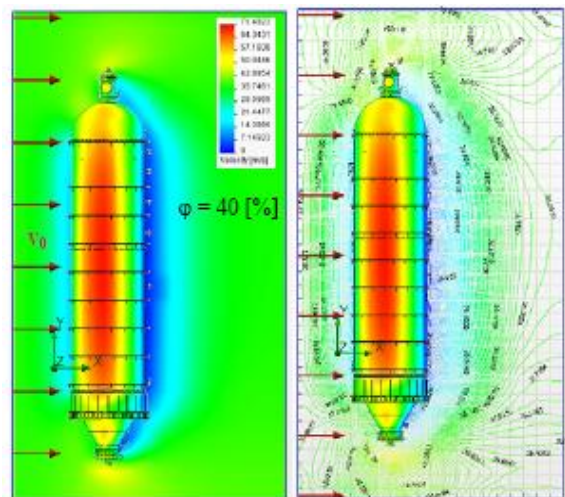


Fig. 19. The 3D field of velocity in Plane 1



Fig. 20. The 3D field of pressure in Plane 1

Fig. 21. The 3D field of temperature in Plane 1
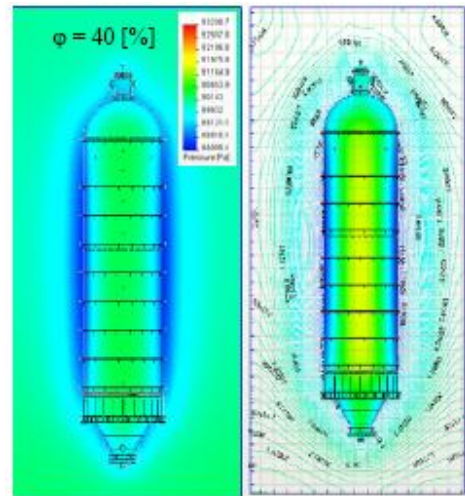


Fig. 24. The 3D field of pressure behind of plant in Plane 2
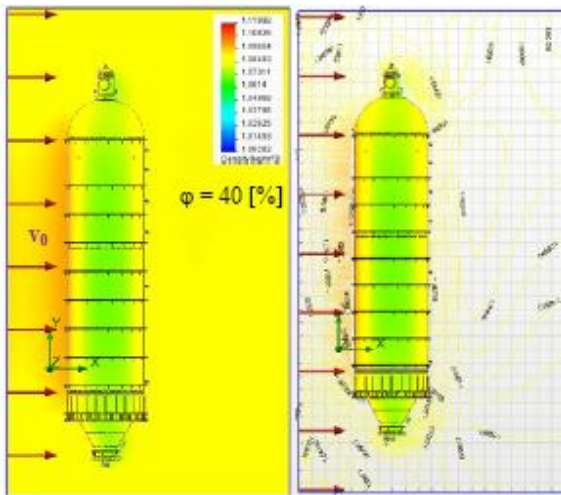


Fig. 22. The 3D field of density in Plane 1
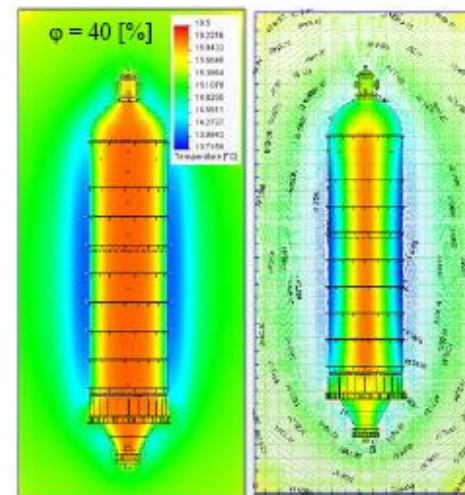


Fig. 25. The 3D field of temperature behind of plant in Plane 2
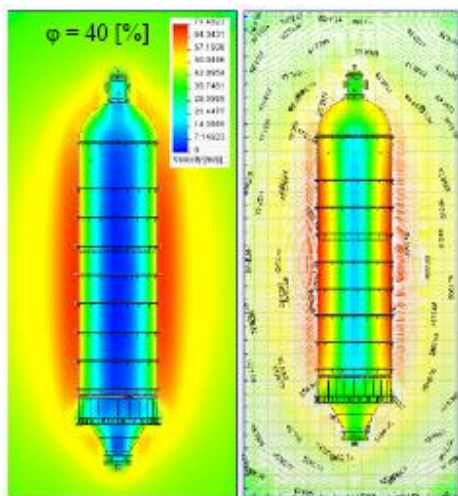


Fig. 23. The 3D field of velocity behind of plant in Plane 2
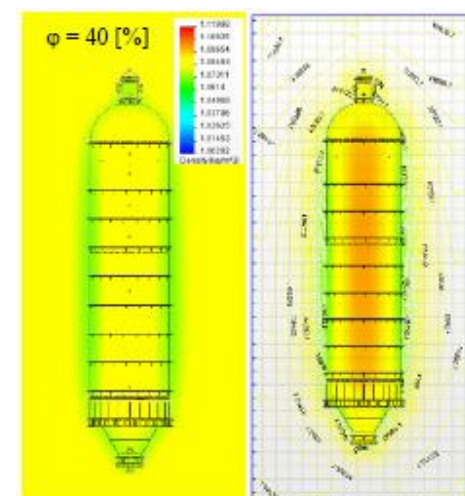


Fig. 26. The 3D field of density behind of plant in Plane 2

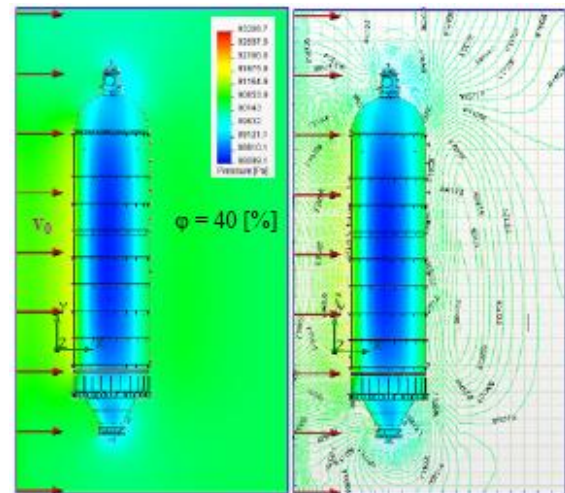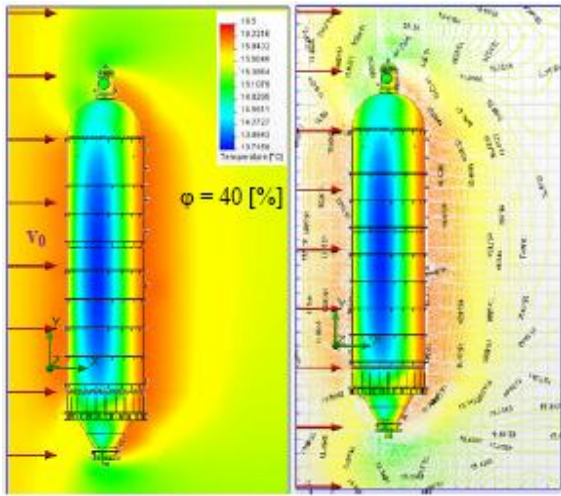The 3D distributions fields contours and isolines of velocity, pressure, temperature and density in horizontal plane through points: $P_1$, $P_5$ and $P_7$ are given in Fig. 27 to Fig. 38.
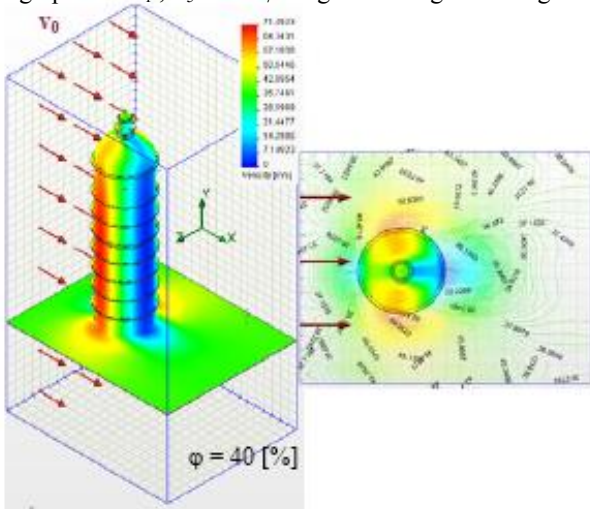


Fig. 27. The 3D velocity's field in horizontal plane through point $P_1$
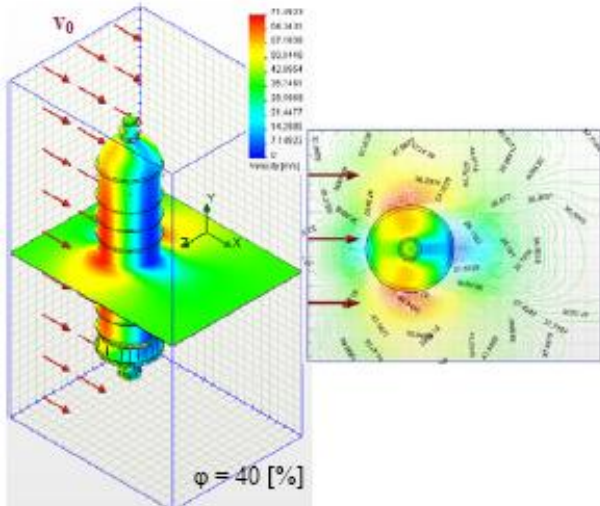


Fig. 28. The 3D velocity's field in horizontal plane through point $P_5$
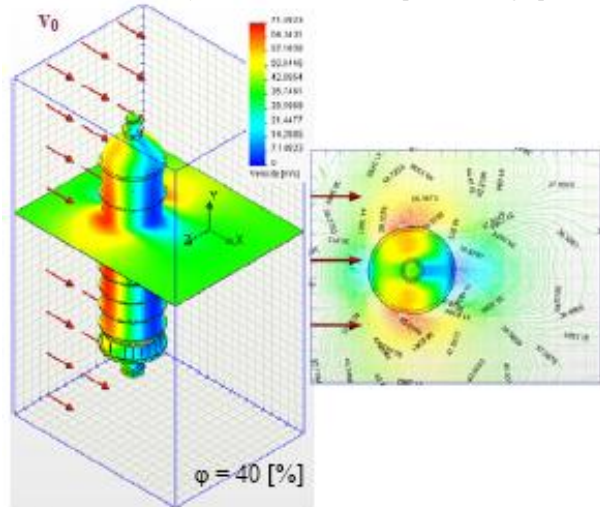


Fig. 29. The 3D velocity's field in horizontal plane through point $P_7$
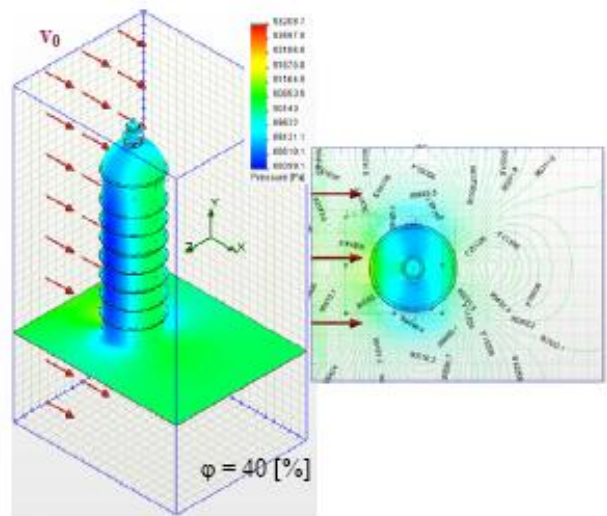


Fig. 30. The 3D pressure's field in horizontal plane through point $P_1$
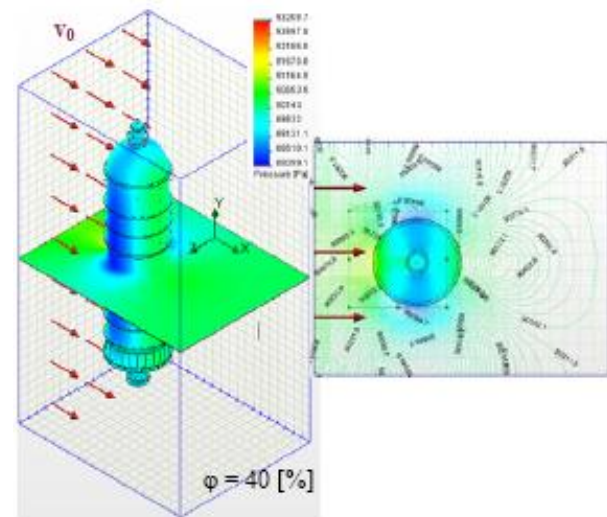


Fig. 31. The 3D pressure's field in horizontal plane through point $P_5$
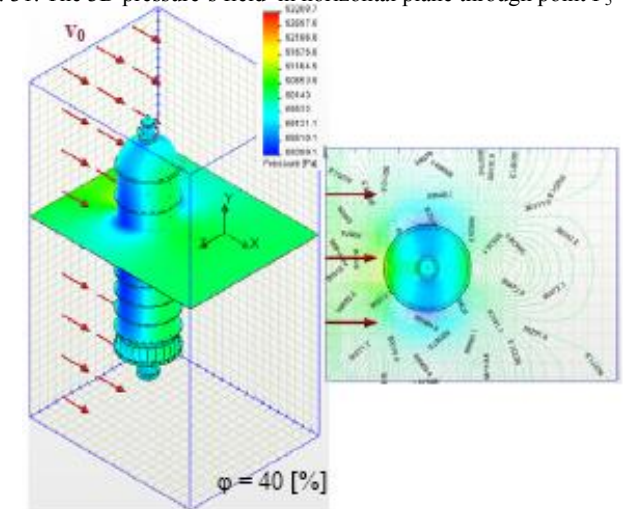


Fig. 32. The 3D pressure's field in horizontal plane through point $P_7$
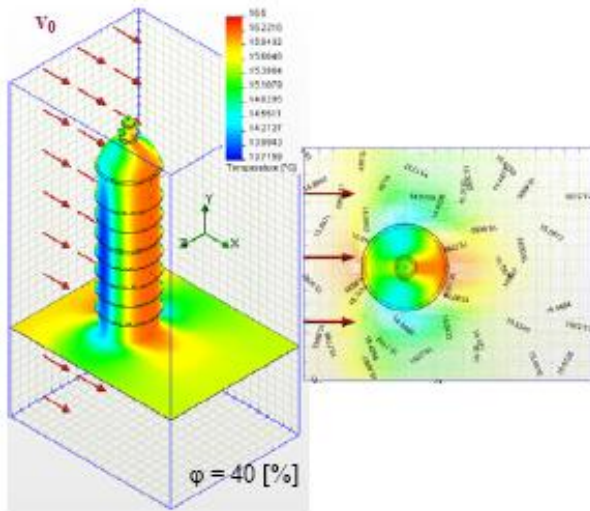
Fig. 33. The 3D temperature's field
in horizontal plane through point $P_1$
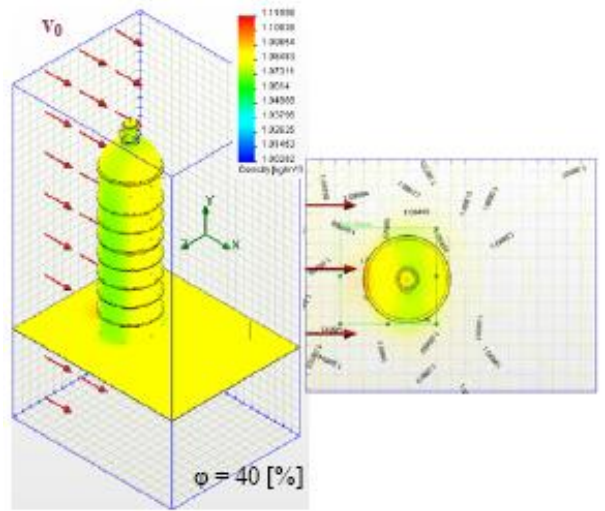


Fig. 36. The 3D density's field
in horizontal plane through point $P_1$
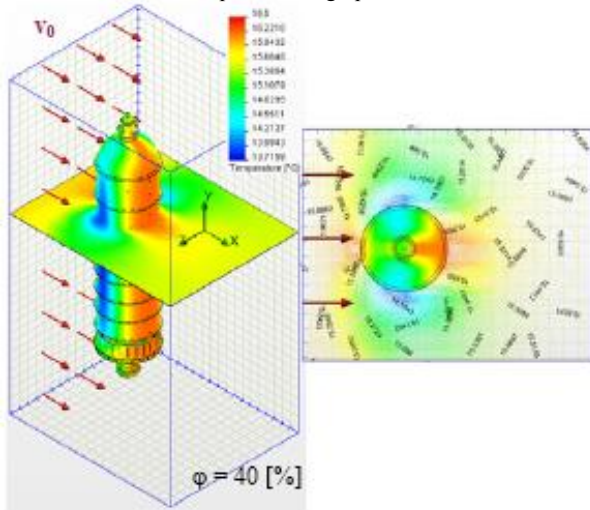


Fig. 34. The 3D temperature's field
in horizontal plane through point $P_5$
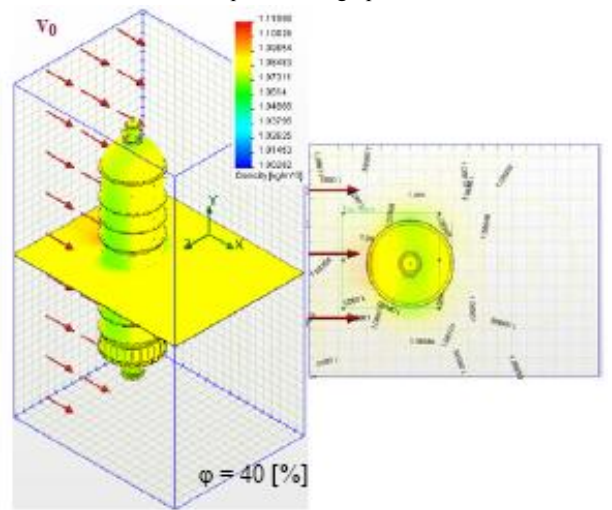


Fig. 37. The 3D density's field
in horizontal plane through point $P_5$
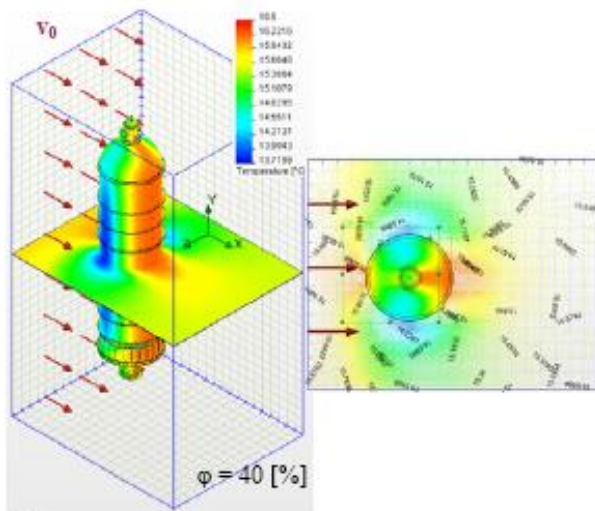


Fig. 35. The 3D temperature's field
in horizontal plane through point $P_7$
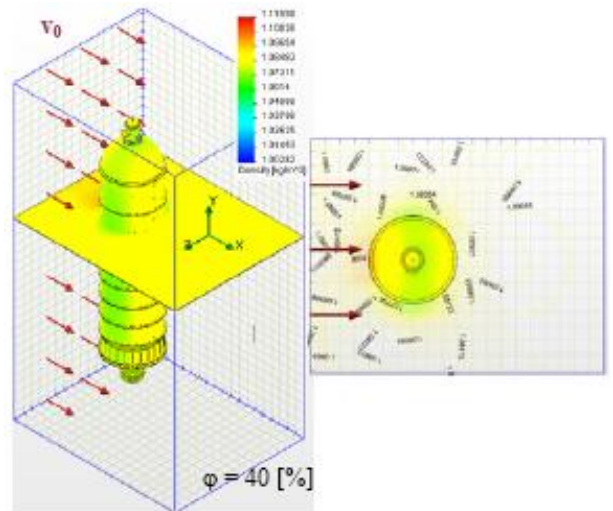


Fig. 38. The 3D density's field
in horizontal plane through point $P_7$
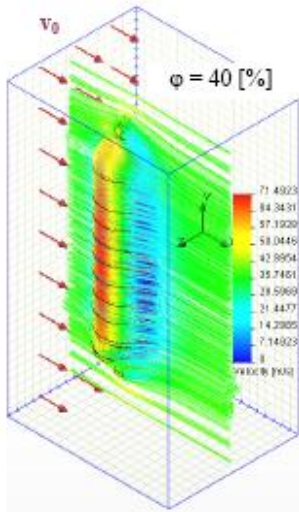
Fig. 39. The 3D trajectory of velocity field
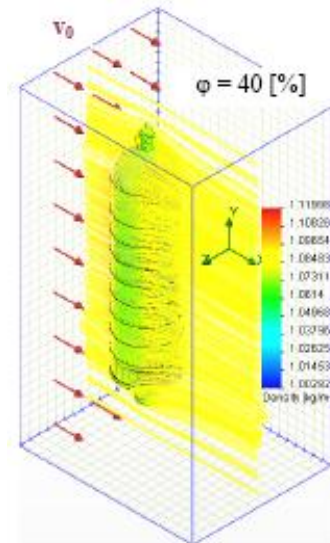


Fig. 42. The 3D trajectory of density field
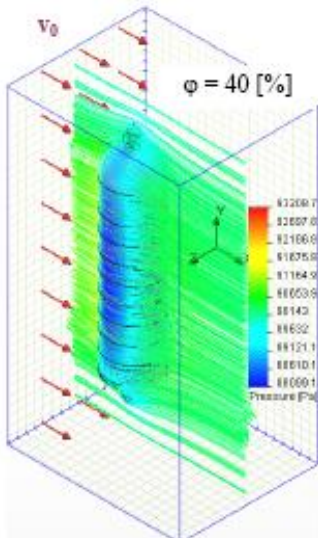


Fig. 40. The 3D trajectory of pressure field



Fig. 43. The deviation of physical sizes calculated in points $P_1$ to $P_9$
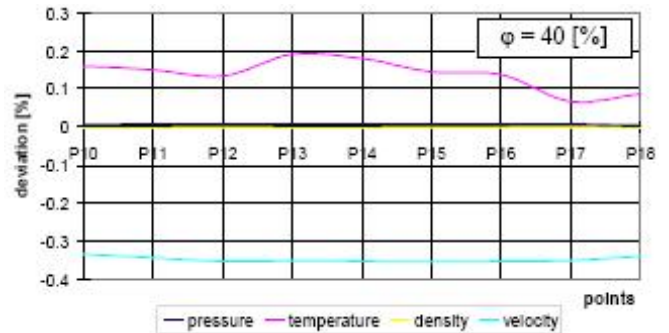


Fig. 44. The deviation of physical sizes calculated in points $P_{10}$ to $P_{18}$



Fig. 41. The 3D trajectory of temperature field
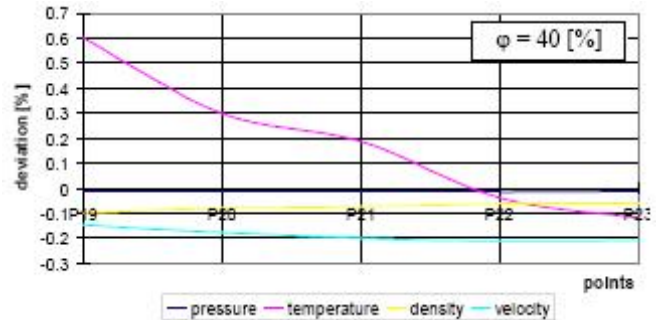


Fig. 45. The deviation of physical sizes calculated in points $P_{19}$ to $P_{23}$

Also the plots of deviation concerning the pressure, temperature, density and velocity, in points $P_1$ to $P_{23}$ at constant humidity $\varphi = 40$ [%], are given in Fig. 43 to Fig. 45.

*4.2.2. The numerical results obtained with the F.E.M*

In present paper the numerical results of simulation are calculated starting at the initial conditions of the experimental measurements for the air front which attacks the plant structure with: p = 90330 [Pa], T = 16 [°C], v = 34,5 [m/s], $\varphi = 40$ [%].
The numerical results of simulation are given in Table 1.

Table 1. The numerical results of simulation concerning the physical sizes of air in points $P_1$ to $P_{23}$.

| points | p [Pa] | T [$^0$C] | $\rho$ [kg/m$^3$] | v [m/s] |
|---|---|---|---|---|
| | with $\varphi = 40$ [%] constant | | | |
| $P_1$ | 90386.25 | 16.2199 | 1.08708 | 4.293 |
| $P_2$ | 90410.25 | 16.2242 | 1.08761 | 3.413 |
| $P_3$ | 90373.01 | 16.2256 | 1.08741 | 2.898 |
| $P_4$ | 90372.57 | 16.2272 | 1.08766 | 2.591 |
| $P_5$ | 90359.35 | 16.2264 | 1.08776 | 2.564 |
| $P_6$ | 90334.28 | 16.2259 | 1.08771 | 2.851 |
| $P_7$ | 90360.48 | 16.2255 | 1.08829 | 3.178 |
| $P_8$ | 90369.97 | 16.2229 | 1.08867 | 3.808 |
| $P_9$ | 90319.90 | 16.1988 | 1.08857 | 7.379 |
| $P_{10}$ | 88945.26 | 14.3631 | 1.07664 | 61.438 |
| $P_{11}$ | 88664.41 | 14.1472 | 1.07430 | 64.839 |
| $P_{12}$ | 88542.59 | 14.0449 | 1.07346 | 66.423 |
| $P_{13}$ | 88477.79 | 14.0013 | 1.07310 | 67.145 |
| $P_{14}$ | 88453.40 | 13.9900 | 1.07311 | 67.318 |
| $P_{15}$ | 88456.51 | 13.9998 | 1.07336 | 67.094 |
| $P_{16}$ | 88497.79 | 14.0567 | 1.07391 | 66.265 |
| $P_{17}$ | 88587.32 | 14.1500 | 1.07490 | 64.677 |
| $P_{18}$ | 88953.84 | 14.5083 | 1.07842 | 58.949 |
| $P_{19}$ | 91307.75 | 16.1502 | 1.09800 | 17.180 |
| $P_{20}$ | 91456.07 | 16.1769 | 1.10021 | 13.079 |
| $P_{21}$ | 91457.27 | 16.1671 | 1.10077 | 12.796 |
| $P_{22}$ | 91399.12 | 16.1444 | 1.10067 | 12.946 |
| $P_{23}$ | 91052.55 | 16.0153 | 1.09760 | 20.801 |

V. THE EXPERIMENTAL MEASUREMENTS

The results of experimental measurements in points $P_1$ to $P_{23}$ concerning the aerodynamically flow are given in Table 2.

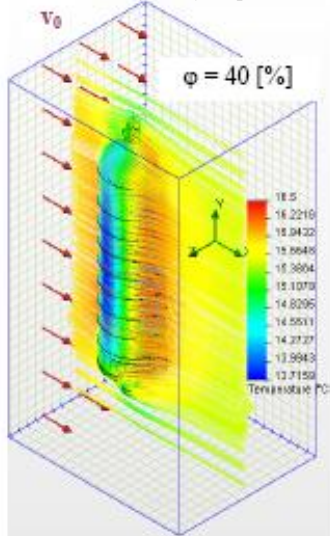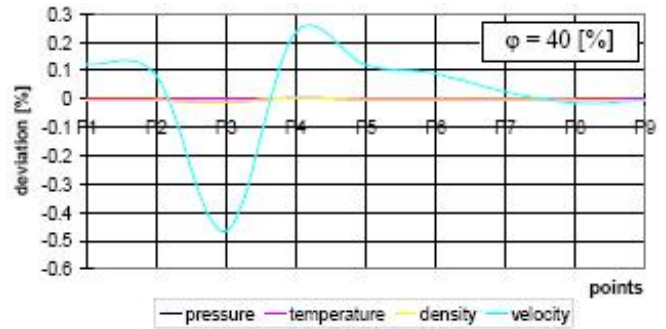Table 2. The numerical results of experimental measurements concerning the physical sizes of air in points $P_1$ to $P_{23}$.

| points | p [Pa] | T [$^0$C] | $\rho$ [kg/m$^3$] | v [m/s] |
|---|---|---|---|---|
| | with $\varphi = 40$ [%] constant | | | |
| $P_1$ | 89261.55 | 16.0497 | 1.06561 | 4.207 |
| $P_2$ | 88872.75 | 16.0397 | 1.06367 | 3.337 |
| $P_3$ | 88740.19 | 16.0284 | 1.06285 | 2.842 |
| $P_4$ | 88644.01 | 16.0379 | 1.05989 | 2.536 |
| $P_5$ | 88518.17 | 15.9992 | 1.06455 | 2.503 |
| $P_6$ | 88441.62 | 15.9829 | 1.06035 | 2.785 |
| $P_7$ | 88380.75 | 15.9574 | 1.0605 | 3.095 |
| $P_8$ | 87686.76 | 15.9894 | 1.06513 | 3.716 |
| $P_9$ | 87825.65 | 15.9405 | 1.06243 | 7.207 |
| $P_{10}$ | 87613.53 | 14.1983 | 1.05397 | 60.274 |
| $P_{11}$ | 87062.46 | 13.9988 | 1.04953 | 63.492 |
| $P_{12}$ | 87216.89 | 13.8893 | 1.05117 | 64.891 |
| $P_{13}$ | 86776.96 | 13.8188 | 1.04784 | 65.494 |
| $P_{14}$ | 86490.07 | 13.805 | 1.04754 | 65.727 |
| $P_{15}$ | 86315.87 | 13.8051 | 1.04636 | 65.368 |
| $P_{16}$ | 86070.59 | 13.838 | 1.04628 | 64.453 |
| $P_{17}$ | 86057.23 | 13.9189 | 1.04308 | 62.677 |
| $P_{18}$ | 86012.22 | 14.2475 | 1.04437 | 57.082 |
| $P_{19}$ | 90118.18 | 15.97132 | 1.07552 | 16.824 |
| $P_{20}$ | 89697.98 | 15.9472 | 1.07421 | 12.815 |
| $P_{21}$ | 89523.56 | 15.9187 | 1.07671 | 12.470 |
| $P_{22}$ | 89274.38 | 15.8558 | 1.06996 | 12.592 |
| $P_{23}$ | 88297.66 | 15.7228 | 1.07062 | 20.299 |

VI. THE ERROR OF THEORETICAL CALCULUS

The error of theoretical calculus concerning the physical sizes calculated and measured in points $P_1$ to $P_{23}$ are given in Table 3. The formula of calculus error is:

$$\varepsilon = \frac{PS_{theoretical} - PS_{experimental}}{PS_{experimental}} \times 100 \ [\%]$$

where PS represents the physical size as: pressure. temperature, density and velocity attach of air.

Table 3. The error of calculus concerning the physical sizes of air calculated in points $P_1$ to $P_{23}$ .

| points | $\varepsilon_p$ [%] | $\varepsilon_T$ [%] | $\varepsilon_\rho$ [%] | $\varepsilon_v$ [%] |
|---|---|---|---|---|
| | with $\varphi = 40$ [%] constant | | | |
| $P_1$ | 1.26 | 1.06 | 2.01 | 2.04 |
| $P_2$ | 1.73 | 1.15 | 2.25 | 2.28 |
| $P_3$ | 1.84 | 1.23 | 2.31 | 1.97 |
| $P_4$ | 1.95 | 1.18 | 2.62 | 2.17 |
| $P_5$ | 2.08 | 1.42 | 2.18 | 2.44 |
| $P_6$ | 2.14 | 1.52 | 2.58 | 2.37 |
| $P_7$ | 2.24 | 1.68 | 2.62 | 2.68 |
| $P_8$ | 3.06 | 1.46 | 2.21 | 2.48 |
| $P_9$ | 2.84 | 1.62 | 2.46 | 2.39 |
| $P_{10}$ | 1.52 | 1.16 | 2.15 | 1.93 |
| $P_{11}$ | 1.84 | 1.06 | 2.36 | 2.12 |
| $P_{12}$ | 1.52 | 1.12 | 2.12 | 2.36 |
| $P_{13}$ | 1.96 | 1.32 | 2.41 | 2.52 |
| $P_{14}$ | 2.27 | 1.34 | 2.44 | 2.42 |
| $P_{15}$ | 2.48 | 1.41 | 2.58 | 2.64 |
| $P_{16}$ | 2.82 | 1.58 | 2.64 | 2.81 |
| $P_{17}$ | 2.94 | 1.66 | 3.05 | 3.19 |
| $P_{18}$ | 3.42 | 1.83 | 3.26 | 3.27 |
| $P_{19}$ | 1.32 | 1.12 | 2.09 | 2.12 |
| $P_{20}$ | 1.96 | 1.44 | 2.42 | 2.06 |
| $P_{21}$ | 2.16 | 1.56 | 2.23 | 2.61 |
| $P_{22}$ | 2.38 | 1.82 | 2.87 | 2.81 |
| $P_{23}$ | 3.12 | 1.86 | 2.52 | 2.47 |

## VII. CONCLUSIONS

Through experimental measurements and theoretical calculus on finding that the 3D distribution fields of physical size which characterize the dynamical flow around the plant structure are no uniform.

The influence of humidity if $\varphi = 0 \div 100$ [%] given the results from Fig. 3 to fig.14 and the Table 4.

Table 4. The minimum and maximum deviation with humidity of physical sizes of air in points $P_1$ to $P_{23}$

| points | maximum | minimum |
|---|---|---|
| pressure | | |
| $P_1$ to $P_9$ | $P_9$ / 0.005 [%]; $\varphi = 46$[%] | $P_3$ /- 0.0175 [%]; $\varphi = 90$[%] |
| $P_{10}$ to $P_{18}$ | $P_{15}$ / 0.018 [%]; $\varphi = 94$[%] | $P_{18}$ / 0.0025 [%]; $\varphi = 10$[%] |
| $P_{19}$ to $P_{23}$ | $P_{23}$ / -0.028 [%]; $\varphi = 10$[%] | $P_{21}$ /- 0.034 [%]; $\varphi = 94$[%] |
| temperature | | |
| $P_1$ to $P_9$ | $P_9$ / 0.009 [%]; $\varphi = 100$[%] | $P_3$ /- 0.0013 [%]; $\varphi = 90$[%] |
| $P_{10}$ to $P_{18}$ | $P_{13}$ / 0.47 [%]; $\varphi = 82$[%] | $P_{17}$ / 0.020 [%]; $\varphi = 68$[%] |
| $P_{19}$ to $P_{23}$ | $P_{19}$ / 0.82 [%]; $\varphi = 60$[%] | $P_{23}$ /-1 [%]; $\varphi = 100$[%] |
| density | | |
| $P_1$ to $P_9$ | $P_9$ / 0.048 [%]; $\varphi = 43$[%] | $P_3$ /- 0.018 [%]; $\varphi = 92$[%] |
| $P_{10}$ to $P_{18}$ | $P_{17}$ / 0.007 [%]; $\varphi = 68$[%] | $P_{11}$ /- 0.016 [%]; $\varphi = 18$[%] |
| $P_{19}$ to $P_{23}$ | $P_{22}$ / -0.02 [%]; $\varphi = 10$[%] | $P_{19}$ /- 0.17 [%]; $\varphi = 86$[%] |
| velocity | | |
| $P_1$ to $P_9$ | $P_1$ / 0.28 [%]; $\varphi = 90$[%] | $P_3$ /- 0.5 [%]; $\varphi = 43$[%] |
| $P_{10}$ to $P_{18}$ | $P_{10}$ / -0.08 [%]; $\varphi = 10$[%] | $P_{14}$ /- 0.78 [%]; $\varphi = 94$[%] |
| $P_{19}$ to $P_{23}$ | $P_{19}$ / -0.15 [%]; $\varphi = 10$[%] | $P_{22}$ /- 0.44 [%]; $\varphi = 100$[%] |

From Table 4 we can conclude:
- the maximum deviation of pressure $\Delta p < 0.018$ [%];
- the maximum deviation of temperature $\Delta T < 0.82$ [%];
- the maximum deviation of density $\Delta \rho < 0.048$ [%];
- the maximum deviation of velocity $\Delta v < 0.28$ [%];

The maximum deviations is $\Delta < 1$[%] so the influence of humidity is small.

If we analyze the results from Table 4 concerning the error of calculus in case with $\varphi = 40$ [%] we can concluded that the maximum error is $\varepsilon < 3,5$ [%] and the numerical simulation made with aid of FEM gives a good results which can be used with success in practical design, with condition if we make the theoretical hypothesis of a constant uniform front of air which collide with the structure of plant at $\alpha = 90^0$ constant.

REFERENCES

[1] Augnier R.H., "A Fast, Accurate real Gas Equation of State for Fluid Dynamic Analisys Application", *Journal of Fluids Engineering,* 1995.
[2] Bockus S., "Solution of some differential equations of reversible and irreversible thermodynamics", *INTERNATIONAL JOURNAL of MECHANICS,* North Atlantic University Union Publishing House, issue 1, volume 1, 2007, pp. 10-14.
[3] Fersiger J.H., Peric M., *Computational Methods for Fluid Dynamics,* Springer Verlag, 2002.
[4] Hirsh C., *Numerical computation of Internal and External Flows. Computational Methods for Inviscid and Viscous Flows,* vol. 2, John Wiley & Sons, New York, 1984.
[5] Hughes T.J.R., *The finite element method linear static and dynamic finite element analysis,* Prentice-Hall, Inc, Englewood Cliffs, NJ, 1987.
[6] Kiselev, P.G.., *Indreptar pentru calcule hidraulice,* Ed. Tehnica, Bucuresti, 1988.
[7] Malerba M., Argento M., Salviulo A., Rossi G.L., "A boundary layer inspection on a wing profile through high resolution thermography and numerical methods", *WSEAS TRANSACTIONS on FLUID MECHANICS,* WSEAS Press, issue 1, volume 3, Jan. 2008, pp. 18-28.
[8] Patankar S.V., *Numerical Heat Transfer and Fluid Flow,* McGraw-Hill, Washington, New-York, London, 1980.
[9] Popescu F., Panait T., "Numerical modelling and experimental validation of a turbulent separated reattached flow", *INTERNATIONAL JOURNAL of MATHEMATICS AND COMPUTERS IN SIMULATION,* North Atlantic University Union Publishing House, issue 1, volume 1, 2007, pp. 7-11.
[10] Reynolds A.J., *Curgeri turbulente în tehnică,* Editura Tehnică, Bucureşti, 1982.
[11] Reynolds W.C.,"Fundamentals of turbulences for turbulence modeling and simulation", *Lecture Notes for Von Karman Institute,* 1987.
[12] Rizea N., "Contribuţii la calculul de fluaj şi oboseală al învelişurilor subţiri cu aplicaţie la aparatura petrochimică", Teză de doctorat, 2008, Universitatea Petrol–Gaze din Ploieşti, Romania.
[13] Sabbagh-Yazdi S.R., Mastoriakis N.E., Meysami F., "Wind flow pressure load simulation around storage tanks using SGS turbulent model", *INTERNATIONAL JOURNAL of MECHANICS,* North Atlantic University Union Publishing House, issue 2, volume 1, 2007, pp. 39-44.
[14] Spalart P., Allmaras S., "A one-equation turbulence model for aerodynamic flow", American Institute of Aeronautics and Astronautics, 1992.
[15] Ţălu M., Bolcu D., Ţălu Ş., Sipos A, "The dynamic flow air visualization around the petrochemistry petroleum coke plant", *Proceedings of the 9th WSEAS International Conference on AUTOMATION and INFORMATION (ICAI '08),* Bucharest, Romania, June 24-26, 2008, WSEAS Press, pp. 164-169. ISSN: 1790-5117, ISBN: 978-960-6766-77-0.
[16] Ţălu M., Bică M., Albotă E., Ţălu Ş., "The dynamic visualization of the 3D thermal impression generated through the air friction with the petroleum coke plant structure", *Proceedings of the 5th WSEAS / IASME International Conference on ENGINEERING EDUCATION (EE '08),* Heraklion, Greece, July 22-24, 2008, WSEAS Press, pp. 349-354, ISSN: 1790-2769, ISBN: 978-960-6766-86-2.
[17] Ţălu M., Bică M., Nanu Andrei Ghe., Albotă E., Ţălu Ş., Aurelian Ş., "Visualization of dynamic behaviour of a petrochemistry petroleum coke plant under verical various seismic loadings", *Proceedings of the $10^{th}$ WSEAS International Conference on Mathematical and Computational Methods in Science and Engineering (MACMESE'08),* Bucharest, Romania, November 7-9, 2008, WSEAS Press, pp. 88-93, ISSN: 1790-2769, ISBN: 978-960-474-019-2.
[18] **** User guide SolidWorks 2007 software.
[19] **** User guide CosmosFlow 2007 software.
[20] **** User guide Maple 11 software.